Torsional properties of staple fibre plied yarns [1]

D.G. Phillips, Canh-Dung Tran,
CSIRO Materials Science and Engineering
P.O. Box 21, Geelong, VIC 3216
Australia

W.B. Fraser
School of Mathematics and Statistics
The University of Sydney
NSW 2006, Australia

and

G.H.M. van der Heijden
Department of Civil, Environmental and Geomatic Engineering
University College London
Gower Street, London WC1E 6BT, UK

November 9, 2008

Abstract

A mathematical analysis of the mechanical governing equations applying to the torsional behaviour of multi-ply yarns under tension has been carried out. This analysis clearly shows that there are two components, a geometric component that determines the slope or gradient of the torque due to tension and a component that determines the yarn torque at zero applied tension (intrinsic torque) that depends on the fibre number, fibre moduli and diameter as well as the strand structural geometry. The effect of the ratio of the ply twist to the spinning twist of the single strands on the torque properties has been numerically analysed for two, three and four-ply yarns prepared from single 31 tex yarns. The model has been compared with experimental torque data for a range of two-ply yarns plied at different percentages of the singles spinning twist and also with different yarn histories and test environments. The experimental data reflect the trends identified by the model.

1 Introduction

During yarn formation from staple fibres such as wool or cotton by ring spinning the fibres are bent and twisted into approximately helical shapes and an unbalanced torque is created due to the elasticity and geometrical configuration of the fibres. As the yarn is wound onto a bobbin immediately after twist insertion the torque required to keep the yarn in its twisted configuration is supplied by inter-yarn friction as it lies on the bobbin. When the yarn is unwound from this bobbin for further processing this residual unbalanced torque or *twist liveliness* can cause problems such as snarling of the yarn unless the yarn tension is kept sufficiently high at all times during the further processing.

One solution to this difficulty with twist liveliness in *singles* yarns is to process them into a two-ply structure (called two folding) with its twist in the opposite direction to that of the singles yarn. If sufficient ply-twist is inserted it is possible to form a balanced ply structure with zero snarling twist. A simple demonstration of this principle can be performed by holding a length of yarn between your hands and inserting some additional twist into it while holding the yarn straight. When you slowly release the tension and allow the ends of the yarn to approach each other a snarl will form in the yarn, and if you do this carefully you can create a piece of balanced two-ply yarn about half as long as the length of the yarn you started with. This two ply yarn will lie on a table without further snarling (or twist liveliness).

Twist liveliness due to yarn torque is important in textile practice and can be desirable for the formation of highly distorted unbalanced crepe yarns used in woven fabrics or undesirable with yarn torque causing skew/spirality in knitwear and even the break-down of balanced yarn structures in cut-pile carpets. Also multi-ply structures are of recent interest for the purpose of controlling fibre movement, see Tran et al. (2008), Tran and Phillips (2008), and these constructions require the conditions for yarn balance to be established for knitwear and woven fabrics.

In order to determine the effectiveness of processing singles yarns into plied yarns with twist of the opposite handedness in reducing twist liveliness, one of us has recently undertaken a series of experiments in which as-spun singles yarns have been further processed into two and higher ply structures using various ratios of singles to ply twist and then the torque and tension that must be applied to the resulting structure to

hold it in its as-spun plied configuration was measured. A number of experiments are described in Section 3 below.

In recent years there have been a number of theoretical investigations into the mechanics and geometry of plied structures consisting of isotropic elastic rods of uniform circular cross-section that are twisted into uniform n-ply structures in which each rod follows a helical path of the same radius and pitch angle; see for example Fraser and Stump (1998a,b), Neukirch and van der Heijden (2002), and Thompson et al. (2002), where references to earlier work may be found.

In Section 2 we develop the mathematical theory combined with numerical analyses to highlight the effect of several key fibre and yarn properties on the torsional properties of multi-ply yarns. Although the theory has been developed for highly idealised structures, which yarn structures certainly are not, we shall construct a theory that relates adequately to initial experimental results in Section 3, and which gives further insight into the issues of twist liveliness.

2 The Mathematical Formulation

We shall draw our equations from Fraser and Stump (1998b) [1] using their notation except that in the present paper θ will replace their ply angle β since their use of θ as the cylindrical coordinate polar angle (in Equation (32), Fraser and Stump, 1998b) will be replaced by ψ, in agreement with the usage by Neukirch and van der Heijden (2002). Thus, after choosing an orthonormal system of basis vectors $(\mathbf{i}, \mathbf{j}, \mathbf{k})$, where $\mathbf{k}$ is directed along the ply axis, we can write for the position vector of a point on the strand axis as it lies in the ply structure (Fig. 1a)

$$\begin{aligned} \mathbf{R}(s) &= x\,\mathbf{i} + y\,\mathbf{j} + z\,\mathbf{k} = a\cos\psi\,\mathbf{i} + a\sin\psi\,\mathbf{j} + s\cos\theta\,\mathbf{k}, \\ \psi' &= \frac{\sin\theta}{a}, \end{aligned} \tag{2.1}$$

where a is the ply radius and $(\ )' = d(\ )/ds$, s being the distance along the strand axis. Also, in this paper the number of strands in the ply will be n instead of N. With these

[1] The description of the n-ply geometry for $n > 2$ in Fig. 4 and Eqs (30) and (31) of Fraser and Stump (1998b) is in error. The correct description can be found in Neukirch and van der Heijden (2002).

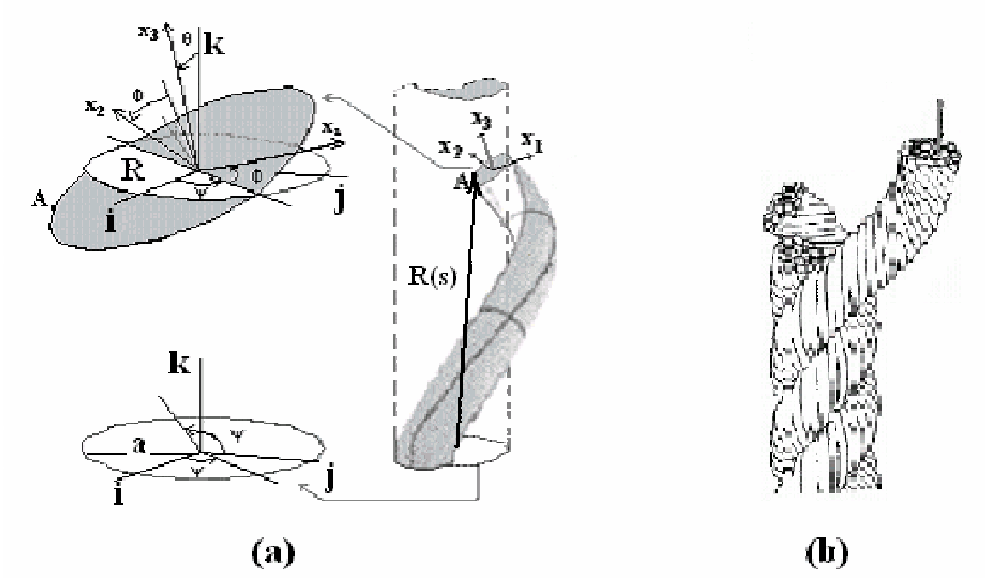

Figure 1: Schematic diagram of a strand wound on a cylinder, showing fixed Cartesian and moving coordinate frames (borrowed from Tran et al. (2007)).

changes the force and moment equilibrium equations for the idealised n-ply structure are given by Equations (34) and (35) of Fraser and Stump (1998a):

$$T_0 = n\left(T\cos\theta + \frac{Q\sin^3\theta}{a} - \frac{B\cos\theta\sin^4\theta}{a^2}\right), \tag{2.2}$$

$$Q_0 = n\left(Ta\sin\theta + Q\cos^3\theta + \frac{B\sin^3\theta(1+\cos^2\theta)}{a}\right), \tag{2.3}$$

where T_0 and Q_0 are respectively the resultant axial tension and torque that must be applied to the n-ply structure in order to maintain it in its as-spun plied configuration. T and Q are the strand tension and torque in the direction tangential to the strand axis, and B is the bending stiffness of the strand. Note that these equations relate to a single layer of rods wrapped on a cylinder of radius a (the radius of the helical path followed by the strand axis). In a two-ply structure this radius is the same as the strand radius.

2.1 Textile yarn twist

Textile yarn twist is measured in turns per metre whereas in the mathematical presentation it is more convenient to express twist in radians per metre. Ply twist and strand

twist will be distinguished as follows.

Ply twist Tw_p is measured in turns per length of the ply axis z so that the strand helix angle in the ply is related to the ply twist by

$$2\pi Tw_p = \frac{d\psi}{dz} = \frac{\tan\theta}{a}. \tag{2.4}$$

Strand twist Tw_s is the twist per unit axial length of the strand and is expressed as follows. For the twist in the straight (pre-twisted) strand before it is spun into the ply structure (ϕ') we shall write

$$2\pi Tw_0 = \phi' = \frac{d\phi}{ds}. \tag{2.5}$$

We call Tw_0 the *spinning twist*. Then for the strand following its helical path as it lies in the ply the strand twist, which is also known as the torsion τ of a strand after creating the ply (Love, 1927), is

$$2\pi Tw_s = \tau = \phi' + \frac{\sin 2\theta}{2a} \tag{2.6}$$

(see Equations (44) and (A.32) in Neukirch and van der Heijden, 2002). Note that all twists are assumed to be right handed in the above equations and that both ply and strand twist are constant in a uniform straight ply.

We now wish to develop a theory relating the force and moment, T_0 and Q_0, required to maintain the plied yarn in its as-spun and plied configuration in terms of the ply and strand twists defined above. In order to do this we need to find a constitutive equation for the strand torque Q_s as a function of the strand torsion and tension τ and T_s.

$$Q_s = F(\tau, T_s). \tag{2.7}$$

2.2 A constitutive equation for strand torque Q_s

Staple fibre yarns (also called strands in this paper) are made by twisting the fibres together (Fig. 1(b)). If each staple fibre is regarded as an elastic rod that is twisted together with other rods so that each rod follows an approximately helical path in the yarn then a very simplified idealised model for this structure can be made by considering the 'singles yarn' to consist of concentric layers of uniform rods of cross-sectional area A_f each following parallel helical paths of helix angle $\beta(r)$ in the layer

of radius r ($0 \leq r \leq R$), where R is the radius of the path of the axes of the outermost layer of fibres in the yarn. This is the idealised geometrical model proposed by Platt et al. (1958), and used by Bennett and Postle (1979a) in their investigations of these structures. More specifically, the rods (fibres) are assumed to be inextensible and their cross-sectional area A_f is assumed rigid so that it doesn't deform as the strand is twisted. We also assume that the rods are smooth so that there is no frictional interaction between adjacent rods. This means that when the yarn structure is twisted the geometrical configuration is preserved with a change in helix angle, and there is no hysteresis due to inter fibre friction in the constitutive equation proposed here. We will use Equations (2.2) and (2.3) to construct a constitutive equation for such a strand. Although these are very unrealistic and restrictive assumptions Bennett and Postle suggest that this model may work for staple fibre yarns where fibre migration can occur during spinning. More problematically we will assume that the applied tension is distributed uniformly in the yarn cross-section, so that concentric layers of rods (fibres) are subjected to a tension that depends on their location $T(r)$. The model for the distribution of fibre tension proposed here lies somewhere between the two 'extreme' models: no fibre migration and perfect migration, proposed by Bennett and Postle (1979a).

Let α replace ψ in this section. First we calculate the number of fibres (rods) dN_f, that lie in the annulus of radius r, width dr and area $2\pi r dr$, where the total number of fibres N_f that make up the yarn is assumed known. If the yarn twist is designated by $\dot{\alpha} \equiv d\alpha/dz = 2\pi T w_s$, where z is distance along the yarn axis, then from Equation (2.4), the helix angle (β) for the fibres in this layer satisfies

$$\tan\beta(r) = r\dot{\alpha} = 2\pi T w_s r. \tag{2.8}$$

This equation, which describes the variation in the helix angle from layer to layer, quantifies the geometrical structure assumed in the model. $\dot{\alpha}$ is the same for all layers.

The cross-sectional area of a fibre that intersects this annulus is $A_f/\cos\beta(r)$, so that the number of fibres that lie in this annulus equals

$$dN_f = \frac{2\pi\cos\beta(r) r dr}{A_f}. \tag{2.9}$$

This equation can now be integrated to obtain an expression for the total number of fibres in the cross-section. In performing this integration it is convenient to use Equation (2.9) as a transformation of the integration variable from r the layer radius,

to $\cos\beta$. Thus

$$N_f = -\int_0^{\beta_s} \frac{2\pi}{A_f\dot{\alpha}^2}\frac{d(\cos\beta)}{\cos^2\beta} = \frac{2\pi}{A_f\dot{\alpha}^2}\left(\frac{1-\cos\beta_s}{\cos\beta_s}\right), \tag{2.10}$$

where β_s is the helix angle of the fibres in the surface layer of the yarn and $\tan\beta_s = R\dot{\alpha}$. When A_f is eliminated between this last equation and Equation (2.9) we obtain

$$dN_f = N_f\left(\frac{\cos\beta_s}{1-\cos\beta_s}\right)\frac{d(\cos\beta)}{\cos^2\beta} \tag{2.11}$$

for the number of fibres in the layer of radius r. We obtain an expression for the strand radius R as a function of the strand twist $\dot{\alpha}$ by using Equation (2.8) to eliminate $\cos\beta$ from Equation (2.9), which after integrating with respect to r and some rearrangement gives

$$R^2 = \frac{(N_f A_f\dot{\alpha})^2}{4\pi^2} + \frac{N_f A_f}{\pi}. \tag{2.12}$$

The first term represents the increase of strand radius due to twist $\dot{\alpha}$. The above results are in agreement with Platt et al. (1959).

We shall assume that the fibres enter the yarn structure with zero pre-twist so that the only torque in the fibres as they lie in the spun yarn is due to the tortuosity of their helical paths (Love, 1927):

$$Q_f(r) = \frac{K_f}{r}\cos\beta(r)\sin\beta(r), \tag{2.13}$$

where K_f is the torsional rigidity of the fibres. The total torque and tension Q_s, T_s acting on the yarn are assumed to be known, so that Equation (2.2) where the bending rigidity of the fibre is B_f can now be used to determine the tension $T_f(r)$ acting on each fibre in the layer of radius r. As mentioned above it will be further assumed that the tension T_s is uniformly distributed across the yarn cross-section. We ignore frictional interaction between the rods (fibres), which may be appropriate for staple fibre yarns, where fibre migration can occur (see, for example, the discussion in Section 2 of Bennett and Postle (1979)). Thus the tension acting on the dN_f yarns in the layer of radius r is

$$\begin{aligned} dT_s &= \frac{T_s 2\pi r dr}{\pi R^2} = \frac{2T_s}{R^2\dot{\alpha}^2}\frac{\sin\beta d\beta}{\cos^3\beta} \\ &= dN_f\left(T_f\cos\beta + \frac{K_f - B_f}{r^2}\cos\beta\sin^4\beta\right), \end{aligned} \tag{2.14}$$

where Equation (2.8) has been used to eliminate r from the last term in the first line of this equation.

The contribution dQ_s of the fibres in this layer to the total torque is obtained from Equation (2.3):

$$dQ_s = dN_f \left[T_f \; r \sin\beta + \frac{K_f}{r} \cos^4\beta \sin\beta + \frac{B_f}{r} \sin^3\beta (1 + \cos^2\beta) \right]. \tag{2.15}$$

Eliminating T_f between these last two equations we obtain

$$\frac{2T_s}{R^2\dot{\alpha}^3} \frac{\sin^3\beta d\beta}{\cos^5\beta} - dQ_s = dN_f \dot{\alpha} \left[K_f \cos\beta (\sin^2\beta - \cos^2\beta) - 2B_f \cos\beta \sin^2\beta \right],$$

where Equation (2.8) has again been used to eliminate r from this last equation. Note also in this derivation that the strand twist $\dot{\alpha}$ is assumed uniform. After substituting expression (2.11) for dN_f into the right hand side of this last equation, it can now be integrated with respect to β, $0 \leq \beta \leq \beta_s$ where $\beta_s = \tan^{-1}(R\dot{\alpha})$ is the value of helix angle β for the fibres in the surface layer of the singles yarn strand. The final result is

$$Q_s = \frac{T_s \tan^4\beta_s}{2R^2\dot{\alpha}^3} + \frac{N_f \dot{\alpha} \cos\beta_s}{1 - \cos\beta_s} \left[(K_f - 2B_f) \log(\cos\beta_s) + (K_f - B_f) \sin^2\beta_s \right], \tag{2.16}$$

where $\tan\beta_s = R\dot{\alpha} = 2\pi RTw_s$. In cases where $|R\dot{\alpha}| << 1$ we may expand the trigonometric functions as follows. First note that Equation (2.8) is exact so that for $|R\dot{\alpha}| << 1$ we have

$$\beta_s = \tan^{-1}(R\dot{\alpha}) \approx R\dot{\alpha}(1 - \frac{1}{3}R^2\dot{\alpha}^2 + \cdots), \tag{2.17}$$

which leads to the following approximations:

$$\begin{aligned} \cos\beta_s &= 1 - \frac{1}{2}R^2\dot{\alpha}^2(1 - \frac{2}{3}R^2\dot{\alpha}^2 + \cdots), \\ \sin\beta_s &= R\dot{\alpha}(1 - \frac{1}{6}R^2\dot{\alpha}^2 + \cdots). \end{aligned}$$

When these approximations are substituted into Equation (2.16) and terms cubic in $\dot{\alpha}$ are retained, we obtain

$$\begin{aligned} Q_s &= \left[N_f K_f + \frac{1}{2}R^2 T_s \right] \dot{\alpha} + N_f \left(B_f - \frac{5}{4}K_f \right) R^2\dot{\alpha}^3 \\ &= \kappa_1\dot{\alpha} + \kappa_3\dot{\alpha}^3, \end{aligned} \tag{2.18}$$

where for the strand lying in the n-ply structure described in the next section, the twist $\dot{\alpha}$ in the above is replaced by the *torsion* τ of the strand lying in a multi-ply yarn (with zero pretwist of fibre) and given in Equation (2.6). Hence, Equation (2.18) is rewritten as

$$Q_s = \kappa_1\tau + \kappa_3\tau^3. \tag{2.19}$$

This is the expression sought in Equation (2.7). We will also require a bending moment/curvature constitutive equation for the strand for which we shall assume the form (cf. Ly and Denby, 1984)

$$\mathbf{M}_s = M_s \mathbf{b}_s + B_s(\mathbf{R}_s{}' \times \mathbf{R}_s{}''), \tag{2.20}$$

where the bending moment (M_s) and rigidity (B_s) of the strand are constants and $\mathbf{b}_s$ is the unit binormal vector to the strand axis (see Fig. 18). Note that the moment/curvature constitutive relation for worsted yarn exhibits significant hysteresis due to inter-fibre friction and the viscoelastic nature of wool fibres. The actual moment curvature relation shown in Figs 2 and 4 of the above reference can be approximated by a parallelogram for which Equation (2.20) with $M_s > 0$ represents the part of the curve on which the bending moment is increasing monotonically with increasing curvature.

2.3 Modelling the n-ply structure

We can now use the strand constitutive relations (2.19) and (2.20) in the force and moment balance equations (2.2) and (2.3) to derive the equilibrium equation for the n-ply.

We assume that the ply is composed of n identical strands whose axes follow a helical path of radius a and helix angle θ. The angular distance between the axes of neighbouring strands is $2\pi/n$. The equations are derived in the Appendix (A.12) and (A.13). Solving these equations for the strand torque and tension we obtain:

$$\begin{aligned} Q_s &= \frac{1}{n\cos 2\theta}\left\{Q_0\cos\theta - aT_0\sin\theta - 2n\left(M_s + B_s\frac{\sin^2\theta}{a}\right)\sin 2\theta\right\}, \\ T_s &= \frac{1}{na\cos 2\theta}\left\{aT_0\cos^3\theta - Q_0\sin^3\theta + n\left(M_s + B_s\frac{\sin^2\theta}{a}\right)\sin^2\theta\right\}. \end{aligned} \tag{2.21}$$

Finally the two expressions (2.21) must be substituted into the strand constitutive Equation (2.19) resulting in

$$\begin{aligned} &-Q_0\left[\cos\theta + \frac{1}{2}\tau R^2\frac{\sin^3\theta}{a}\right] + \left[a\sin\theta + \frac{1}{2}\tau R^2\cos^3\theta\right]T_0 \\ &+2n\left(M_s + B_s\frac{\sin^2\theta}{a}\right)\sin 2\theta + n\tau N_f K_f\cos 2\theta + \frac{n\tau R^2}{2a}\left(M_s + B_s\frac{\sin^2\theta}{a}\right)\sin^2\theta \\ &+nN_f\cos 2\theta\left(B_f - \frac{5}{4}K_f\right)R^2\tau^3 = 0. \end{aligned} \tag{2.22}$$

This equation may be rewritten as

$$\mathcal{K}_0 Q_0 + \mathcal{L}_0 T_0 + \mathcal{M}_0 = 0, \tag{2.23}$$

where

$$\mathcal{K}_0 = -\left(\cos\theta + \frac{\tau R^2 \sin^3\theta}{2a}\right), \tag{2.24}$$

$$\mathcal{L}_0 = \left(a\sin\theta + \frac{\tau R^2 \cos^3\theta}{2}\right), \tag{2.25}$$

$$\begin{aligned}\mathcal{M}_0 = &\left(M_s + B_s\frac{\sin^2\theta}{a}\right)\left(2n\sin 2\theta + \frac{n\tau R^2}{2a}\sin^2\theta\right) \\ &+N_f n\tau K_f \cos 2\theta + nN_f \cos 2\theta\left(B_f - \frac{5}{4}K_f\right)R^2\tau^3,\end{aligned} \tag{2.26}$$

and where θ and τ are calculated from Tw_p and Tw_0 through Equations (2.4) and (2.6) as follows:

$$\begin{aligned}\theta &= \tan^{-1}(2\pi a Tw_p), \\ \tau &= \phi' + \frac{\sin 2\theta}{2a} = 2\pi Tw_0 + \frac{\sin 2\theta}{2a}.\end{aligned}$$

The variables in the above are:

a	the ply radius
R	the strand radius
B_f	the fibre bending rigidity
B_s	the strand bending rigidity
K_f	the fibre torsional rigidity
M_s	the constant moment due to bending hysteresis
n	the number of strands in the ply
N_f	the number of fibres in a strand cross-section
Q_0	the ply torque
T_0	the ply tension
Tw_0	the spinning twist (turns per metre)
Tw_p	the ply twist (turns per metre)

The combination nN_fK_f is essentially the ply torsional stiffness since nN_f is the total number of fibres in a cross-section.

A key result of Equation (2.23) is the resolution of the torque due to tension into two components: the slope of the torque with tension $(-\mathcal{L}_0/\mathcal{K}_0)$ and the torque at zero tension $(-\mathcal{M}_0/\mathcal{K}_0)$, also called the intrinsic torque. The relationships for $\mathcal{L}_0$ and $\mathcal{K}_0$ in Equations (2.24) and (2.25) depend solely on the structural geometry of the yarns,

Table 1: The fibre bending and torsional moduli (mN/mm^2). * Mitchell and Feughelman (1965); ** Speakman (1929).

Test Conditions	Bending*	Torsional**
65%, 20^o C	4.0e6	1.0e6
Wet	1.8e6	1.2e5

namely, the strand helix angle θ, the strand and ply radii R and a, and the torsion τ, and not on any fibre-specific parameters. By contrast the torque at zero tension (see Equation (2.26)) depends on both the ply structural geometry parameters, listed above, and the fibre and yarn mechanical properties, including the fibre and strand torsional and bending rigidities.

2.4 Numerical analysis

In this section an analysis of the above model given by Equation (2.22) is presented. The constant moment due to bending hysteresis (M_s) was initially assumed to be zero and the effect of tension on the spinning twist was assumed to be negligible. Also, the radius of the strand was calculated as a function of the yarn count, packing fraction and fibre density following the approach used in Tran et al. (2007). For example, the packing fraction used for wool worsted yarns was 0.63 with a fibre density of 1.31 g/cm^3 and the single yarn radius was determined using Grosberg's formula (Booth, 1975). Similarly, as described in Tran et al. (2007), the bending rigidity of the single yarn was determined from Ly and Denby (1984) and the ply diameter was calculated from the geometrical governing equations (9a,b) given in Tran et al. (2007). The values of the fibre bending and torsional moduli are shown in Table 1.

For the initial numerical analysis relating to ambient test conditions, 31 tex singles yarns spun in the Z-twist direction from 20.2 μm wool fibres were assumed to be twisted into two-ply 62 tex, three-ply 93 tex and four-ply 124 tex yarns in the S-twist direction with a ply twist Tw_p at 20, 40, 60 and 80% of the original spinning twist Tw_0 of 568 tpm (a twist factor of 100). The results obtained from the model for the R62/2 tex yarns are graphed in Fig. 2 and show that for a specific spinning twist of the single yarn, the ply twist ratio Tw_p/Tw_0 has a significant effect on the slope of

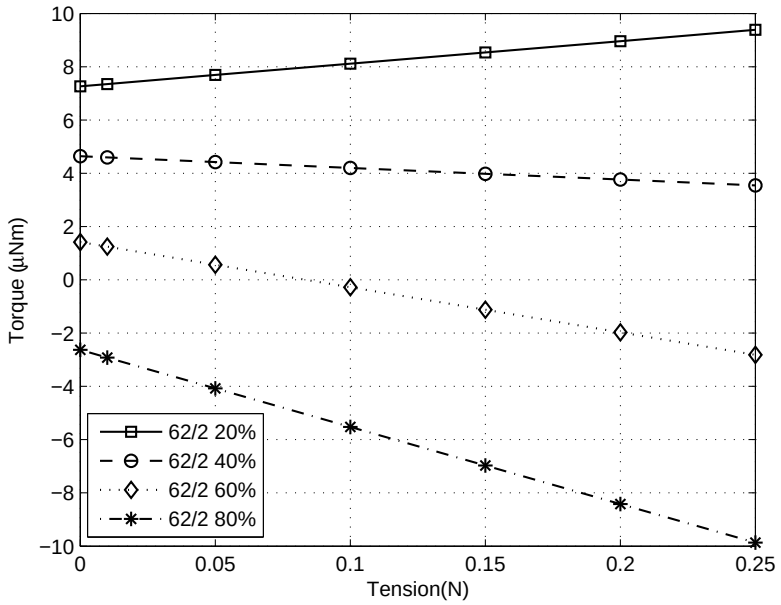

Figure 2: Torque as a function of tension for R62/2 plied yarns with 20%, 40%, 60% and 80% of the spinning twist (568 tpm).

the torque-tension relationship as well as on the intrinsic torque. We can see in Fig. 2 that the slope approaches zero at a ply twist ratio below 40% and the intrinsic torque is zero for a ply twist ratio between 60 and 80%. Note that in this work, the ply twist ratio is expressed as a percentage.

In the following, the slope of the relationship between the torque and the tension ($-\mathcal{L}_0/\mathcal{K}_0$) and the intrinsic torque ($-\mathcal{M}_0/\mathcal{K}_0$) were calculated from Equations (2.23)-(2.26). Fig. 3 shows the torque-tension relationships for three-ply (left) and four-ply (right) yarns respectively. Again the analysis shows that the slope of the torque-tension relationship changes from positive to negative as the ply twist ratio increases and reaches a zero slope for a ply twist ratio below 40% for the three-ply and close to 20% for the four-ply yarn. The effect of the ply twist ratio on the torque-tension slope is shown for an extended range of initial spinning twist from 250 to 1015 tpm, i.e., twist factors from 44 to 179, in Fig. 4 for two-ply (left) and three-ply (right) yarns, respectively. These results confirm that the trends observed in Fig. 3 for one spinning twist apply generally across a very wide range of spinning twists. The influence of the number of strands on the torque-tension slope is summarised in Fig. 5 for two values of ply twist ratio, 20 and 60%. The relative effect of the number of strands is less at

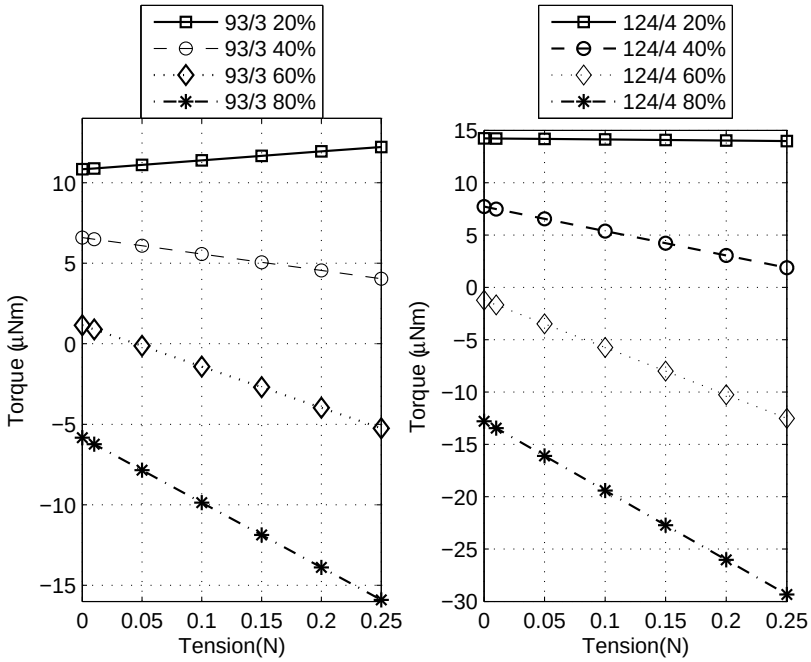

Figure 3: Torque as a function of tension for R93/3 (left) and R124/4 (right) plied yarns, respectively with 20%, 40%, 60% and 80% of the spinning twist (568 tpm).

the lower ply twist ratio.

The effect of ply twist ratio on the slope of the torque-tension relationship for R62/2 yarns is summarised in Fig. 6 and shows that the point of zero slope occurs at 33% ply twist ratio and is clearly independent of the yarn spinning twist. Model values are also shown for an R160/2 yarn, singles twist factor 100 or 354 tpm, and this also intersects the x axis at 33% ply twist ratio. Other calculations from the model show that the point of intersection at 33% is independent of the packing fraction value used in the analysis. The calculations are independent of the fibre properties and dependent on the yarn geometry, see Equations (2.24) and (2.25).

The effect of the ply twist ratio on the intrinsic torque is related to the initial spinning twist in Fig. 7 for two-ply (left) and three-ply (right) yarns, respectively. The results show that the ply twist required for zero intrinsic torque varies with the spinning twist, e.g., at 450 tpm the ply twist value for zero torque is near 80% but is less than 60% for a spinning twist of 850 tpm.

The influence of the number of strands on the intrinsic torque is given in Fig. 8 for

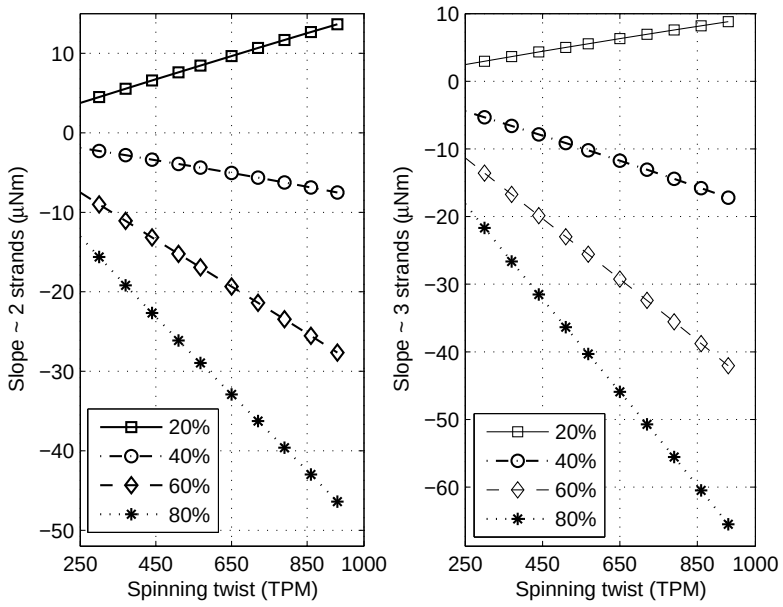

Figure 4: Slope of torque-tension as a function of spinning twist for R62/2 (left) and R93/3 (right) multi-ply yarns with 20%, 40%, 60% and 80% of the spinning twist.

two ply twist ratios, 20 and 60%. The results obtained from the model for the 60% ply twist ratio show that the point of zero intrinsic torque depends on the spinning twist and the number of plies.

The influence of fibre and strand torsional and bending rigidity on the intrinsic torque was also considered by comparing two-ply yarns spun from 17 μm and 20.2 μm fibres, and this is shown in Fig. 9. The effect of the finer fibres is to reduce the intrinsic torque.

Yarn hysteresis is difficult to measure, particularly on unsteamed and twist lively yarns and M_s was assumed to be zero in the preceding calculations. Further numerical analysis using the model shows that M_s can influence the zero torque conditions. Limited published data by Dinghra and Postle (1976) give values for 60 tex singles from 28.5 μm wool of 0.3 μNm (unsteamed) and 0.2 μNm (steamed) measured in ambient conditions. Measurements were made in the present study on 80 tex, 20.2 μm wool, steamed singles yarns using KESF bending equipment in both ambient and wet conditions. The values of the bending moment changed with yarn twist with mean values about 0.28 μNm(ambient) and 0.34 μNm(wet). In the calculated data shown in Figs 10 and 11 a

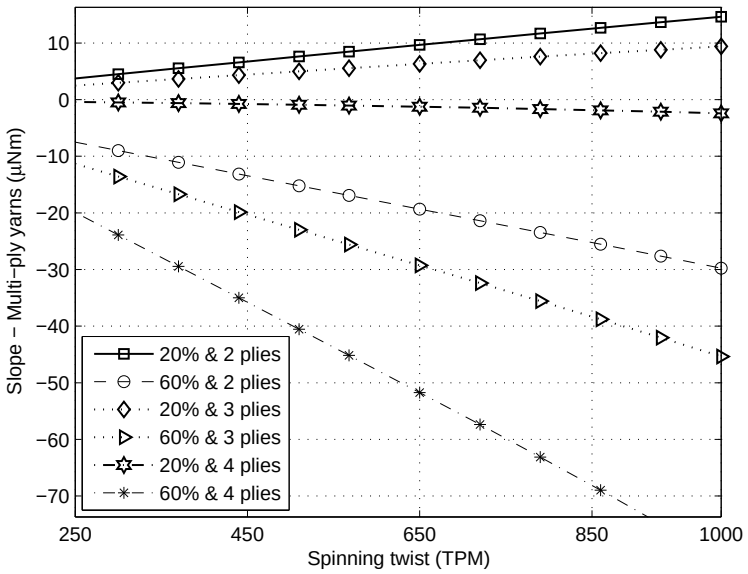

Figure 5: Slope of torque-tension as a function of spinning twist for multi-ply yarns of 2,3,4 strands with 20% and 60% of the spinning twist.

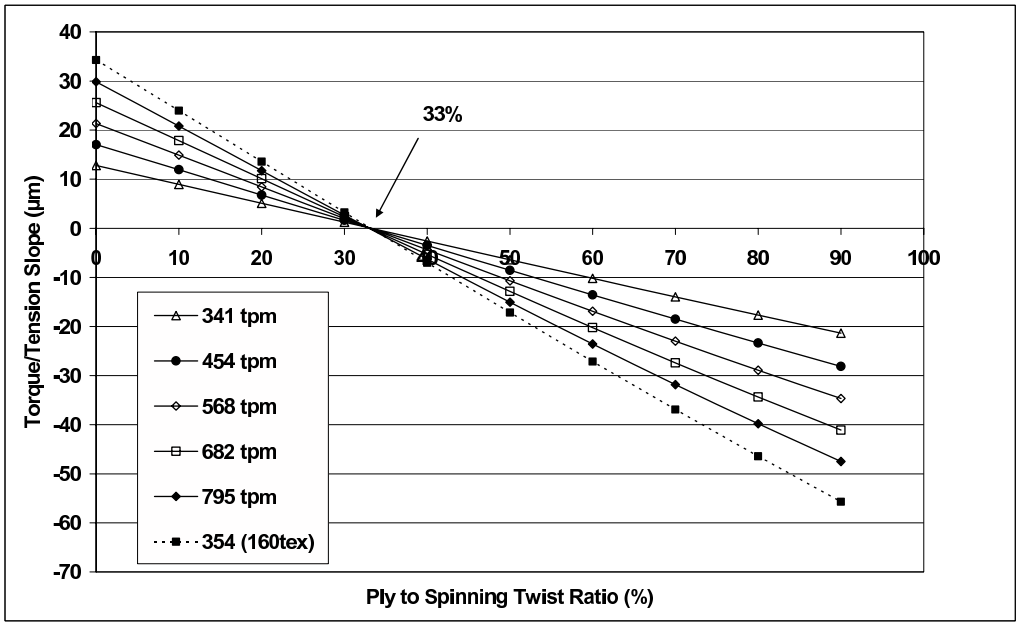

Figure 6: Slope of torque-tension as a function of ply twist ratio for different yarn spinning twists and yarn counts.

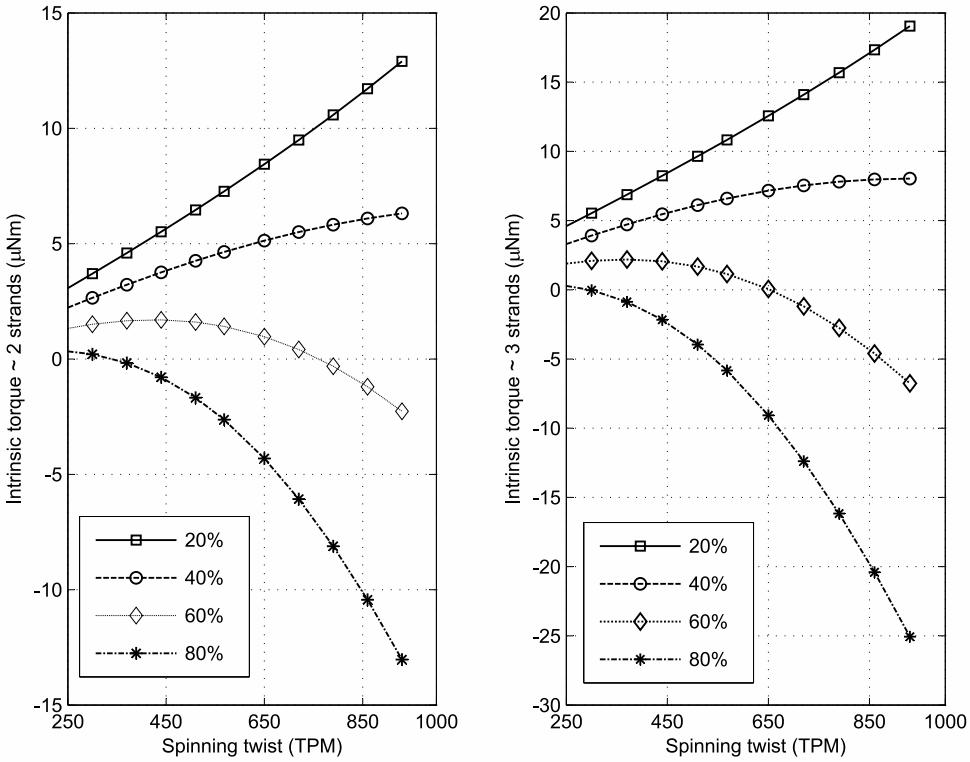

Figure 7: Intrinsic torque as a function of spinning twist for R62/2 (left) and R93/3 (right) plied yarns with 20%, 40%, 60% and 80% of the spinning twist.

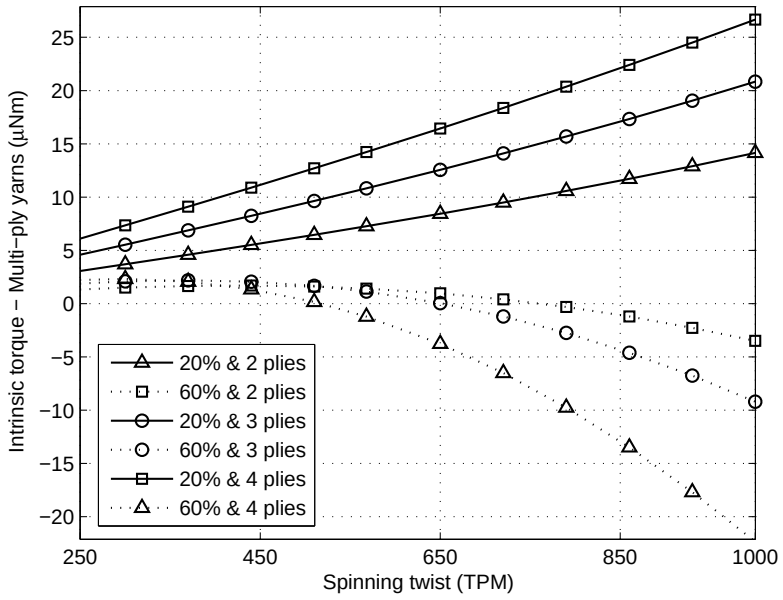

Figure 8: Intrinsic torque as a function of spinning twist for multi-ply yarns of 2,3,4 strands with 20% and 60% of the spinning twist.

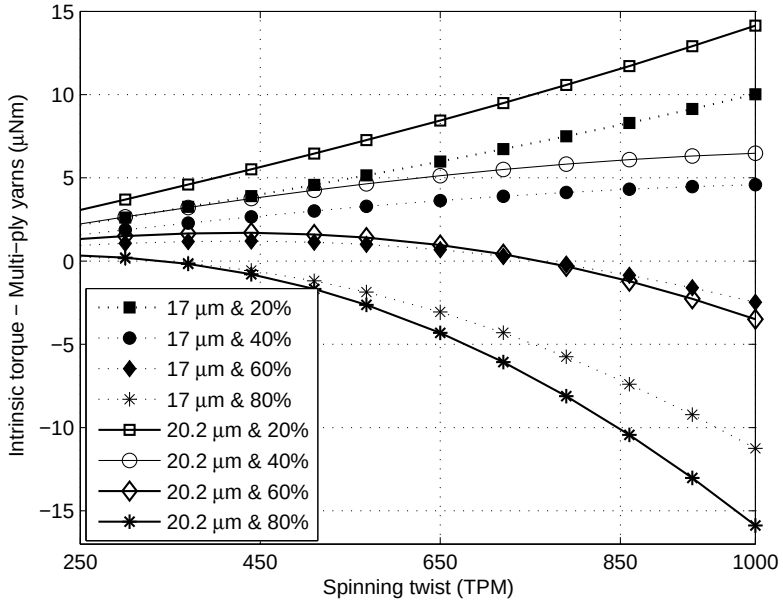

Figure 9: Influence of the fibre diameter (17μm and 20.2μm) on the intrinsic torque for the two-ply yarns with 20%, 40%, 60% and 80% of the spinning twist.

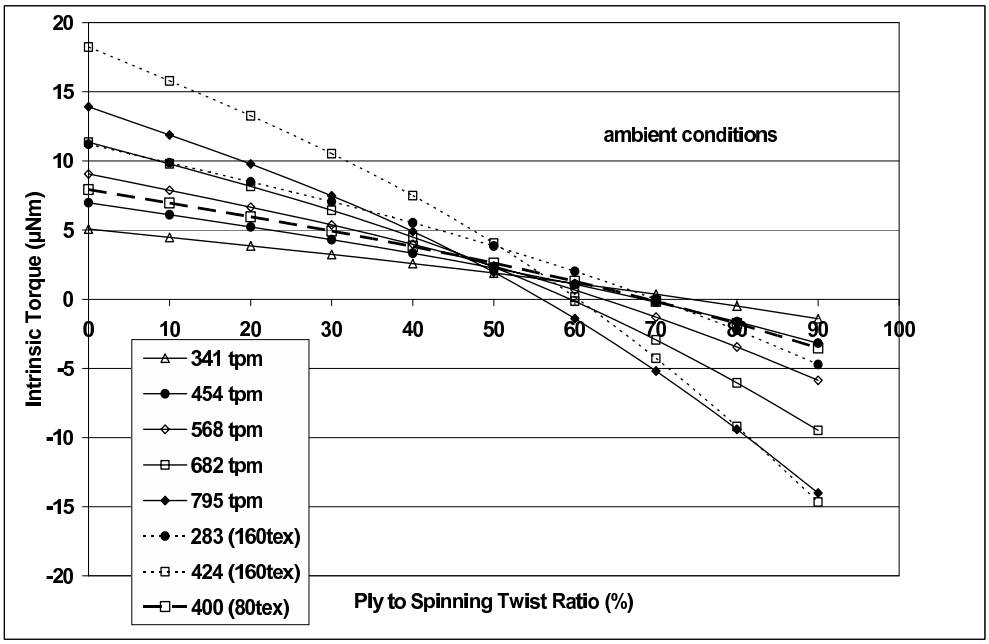

Figure 10: Intrinsic torque as a function of ply twist ratio for different yarn spinning twists and yarn counts.

constant value of 0.3 μNm for the yarn bending moment M_s has been used for both the ambient and wet conditions.

The effect of the ply twist ratio on the ambient intrinsic torque (65% r.h., 20C) for the R62/2 yarns was calculated ($-\mathcal{M}_o/\mathcal{K}_o$) and is shown in Fig. 10 for the spinning twists from 341 tpm to 795 tpm (singles twist factors of 60 to 140). The ply twist ratio for zero torque varies from about 56 % to 74 % increasing as the singles spinning twist decreases. Some calculated data are shown for R160/2 yarns, one with a singles twist factor 80 or 283 tpm and the other with a singles twist factor of 120 or 424 tpm. Calculated data are also shown for R80/2 yarns with a ply twist ratio of 69% for zero torque. These data show a region of ply twist ratio around 48-52% where the intrinsic torque is similar for two-ply constructions from similar yarns, that is, a ply twist ratio of 48-52% defines a region of plied yarn isotorque.

For comparison with Fig. 10, the numerical analysis for the effect of the ply twist ratio on the intrinsic torque of two-ply R62/2 tex yarns is shown in Fig. 11 for wet test conditions using the wet mechanical fibre data given in Table 1.

The ply twist ratio for zero torque shows values from about 41% to 46%, increasing

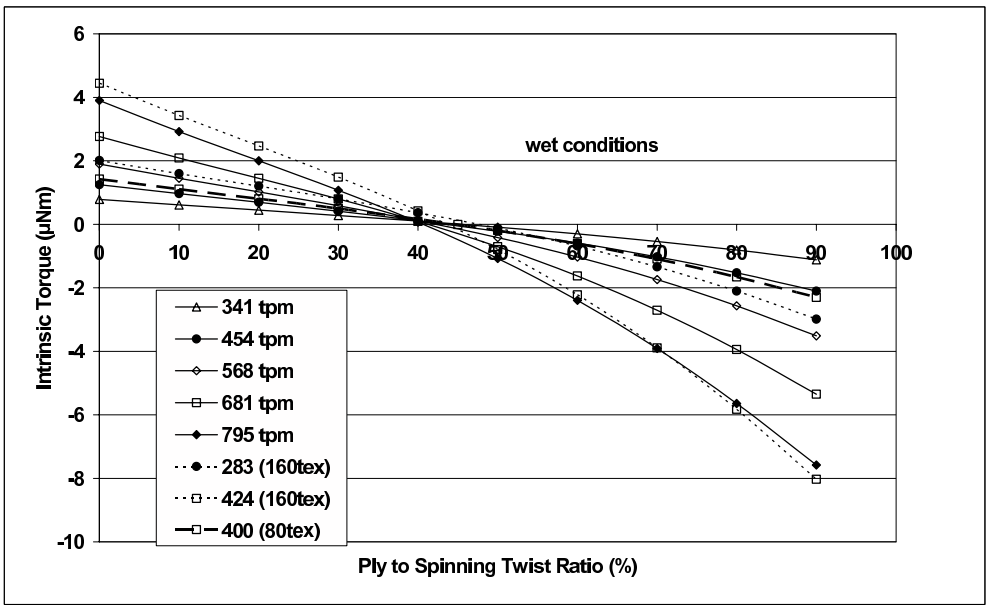

Figure 11: Intrinsic torque as a function of ply twist ratio for different singles yarn spinning twists and yarn counts.

as the singles spinning twist decreases and lower than in the dry case given in Fig.10. The values for the intrinsic torque in the plied yarns is much lower than in the dry case due to the reduction in the fibre bending and torsional stiffness in the wet conditions. The calculated data for R160/2 yarns show similar reductions in intrinsic torque and for the R80/2 yarns the ply twist ratio for zero torque is 45%. The point of isotorque for the wet two-ply yarns occurs at a ply twist ratio near 40%, lower than observed for the dry conditions in Fig.10.

3 Investigation and Discussion

3.1 Experimental method used to measure the torque in two-ply yarns

As described previously by Mitchell et al. (2006) a torquemeter was constructed to directly measure the torque in the hanks of yarn. Weights were applied to the hank manually and the torque of the hank was measured. The work by Mitchell et al. (2006) showed that the torque per strand was independent of the number of strands in the hank and the hank length. For the present study a hank of loop length 400 mm comprising 5 loops was prepared and attached to the torsion wire, that is, 10 strands each of 200 mm in length were measured. The slope of the relationship between the torque per strand and the tension per strand and the intercept at zero tension, the intrinsic torque, were calculated from the line of best fit which had a coefficient of correlation above 0.96. The hanks were attached to the torquemeter and tested at standard conditions, 65% r.h., $20°C$, or allowed to soak for 15 minutes before testing while wet. The tension applied to the wet hank was corrected for buoyancy effects.

In contrast to earlier studies on single yarns by Mitchell et al. (2006), this work measured the torque generated in the yarns after plying. The single yarns were plied using ply twists chosen as a percentage of the initial spinning twist, using a range to cover the value of 55 %, which is commonly chosen as the point of yarn balance.

3.2 Results and discussion

The following yarns in this study were spun from untreated, undyed wool tops with a mean fibre diameter of 20.2 μm and a coefficient of variation (CVD%) of 18.9.

Single yarns were ring-spun with Z-twist to a yarn count of 31 tex with spinning twists of 341, 454, 568, 682 and 795 tpm or twist factors of 60, 80, 100, 120 and 140 respectively (twist factor is defined as tpm(yarn count)$^{1/2}$ where tpm is the turns per metre and yarn count is in kilotex). After spinning, the yarns were steamed on the spinning packages at 87°C for 2 cycles of 5 minutes.

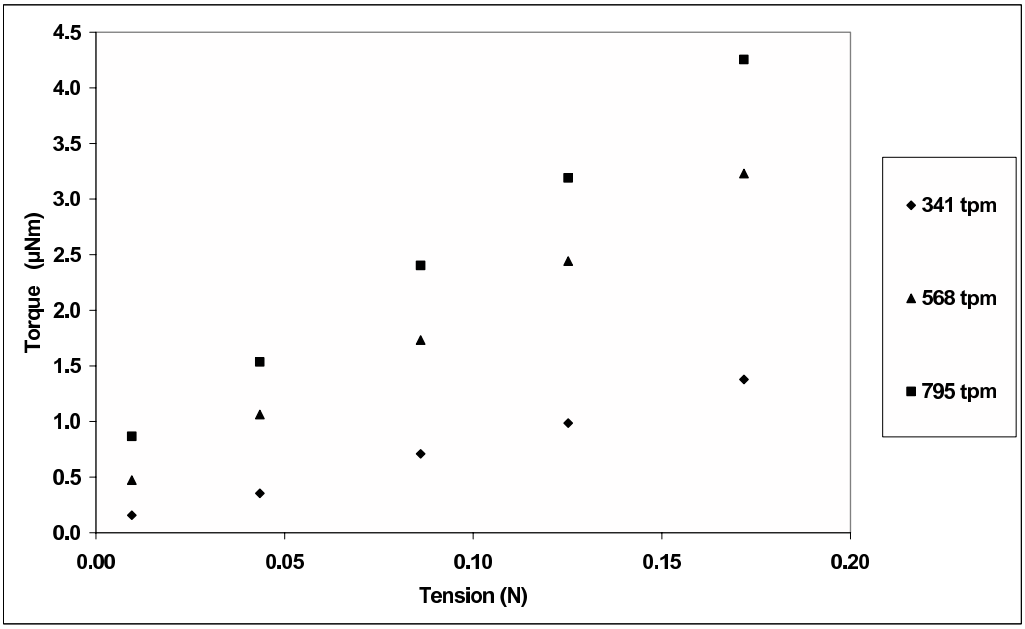

Figure 12: The torque as a function of tension of single 31 tex yarns spun at three spinning twists.

A typical set of results (wet) for steamed singles yarn, ring-spun to 31 tex from 20.2 μm wool with spinning twists of 341, 568 and 795 tpm is shown in Fig. 12. The data show that the slope of the torque due to tension and the intrinsic torque increases with yarn twist as detailed elsewhere (Tran and Phillips, 2007).

The 31 tex single yarns were twisted into two-ply 62 tex yarns in the S-twist direction, steamed and the torque was measured wet for different levels of ply twist. An example is shown in Fig. 13 for the as-spun 31 tex, 100 twist factor yarns (568 tpm) and after plying at 40, 50, 60 and 70% of the original spinning twist.

Interestingly, the commonly accepted ply twist ratio for balance of 55% produces a yarn that has a negative intrinsic torque and a negative slope of the torque due to tension. This is discussed below.

The experimental values of the ply twist ratio for the point of zero slope and the point of zero intrinsic torque were estimated by plotting the gradient and intercept given by the lines of best fit (shown in Fig. 13 for the 568 tpm single yarns plied at 40 and 60%) for all the two-ply yarns against the ply twist ratio, see Fig. 14, and shows that the point of zero slope occurs at a ply ratio of about 29 - 36% when extrapolated from

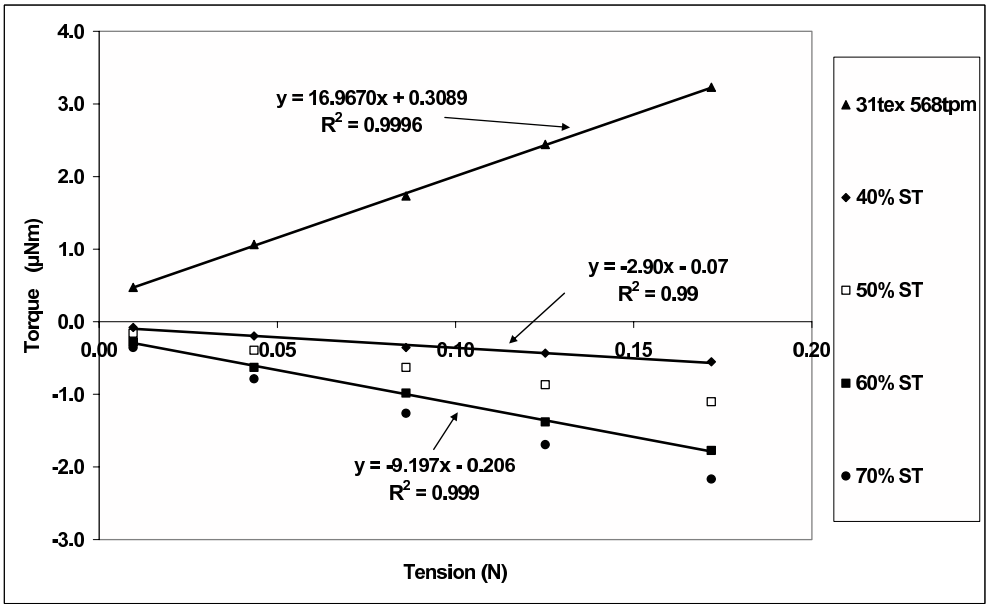

Figure 13: Torque as a function of tension for the R62/2 tex yarns at ply twist ratios of 40%, 50%, 60% and 70% of the singles spinning twist (568 tpm).

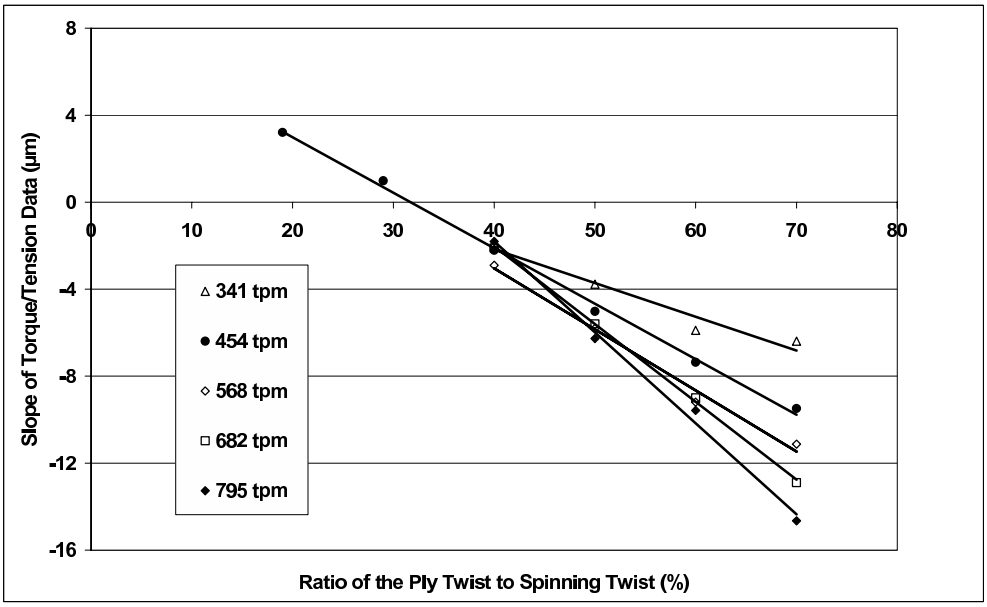

Figure 14: The slope of the torque/tension relationship as a function of the ply twist ratio for two-ply yarns prepared from single yarns of different spinning twist.

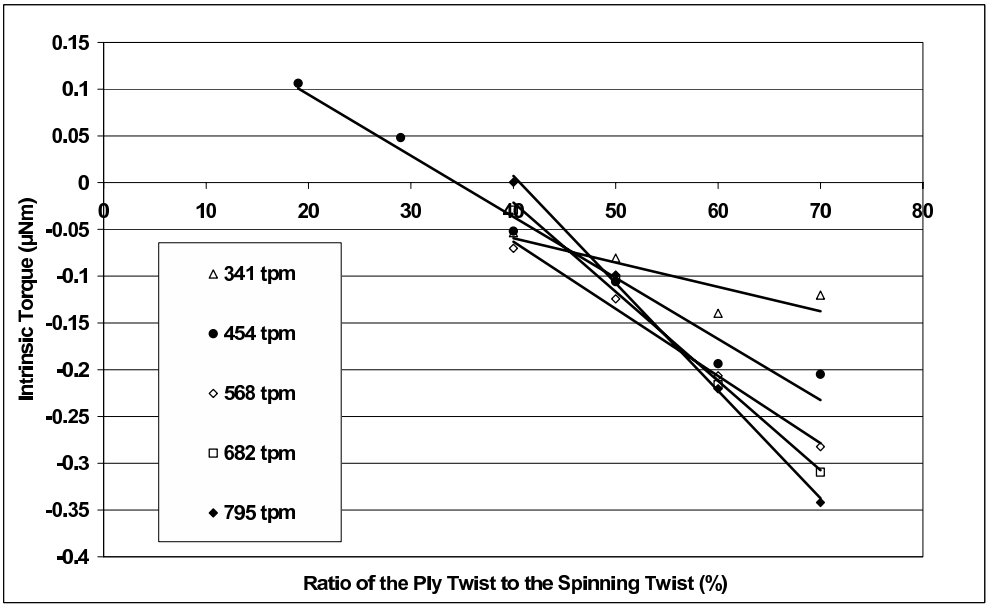

Figure 15: The intrinsic torque as a function of the ply twist ratio for two-ply yarns prepared from single yarns of different spinning twist.

the regression equations. This was measured directly for the 454 tpm twist yarn by preparing additional yarns with ply twist ratios of 19% and 29% and this showed that the point of zero slope occurred at 32%. This value agrees well with the 33% shown in Fig. 6.

However, the experimental values of the slope are about half the calculated values. As pointed out in Section 2.3, the slope depends on the geometry of the ply structure and this discrepancy between the experimental and model-based data suggests that the "effective" strand and ply radii are less than the calculated values. This conclusion is consistent with the single yarn torsional data in Mitchell et al. (2006) where the packing fraction derived from the experimental data was estimated at about 0.9.

The intrinsic torque for the steamed R62/2 tex yarns measured wet are shown in Fig. 15. These torque values are quite small and show some scatter but generally the data indicate that the ply twist for zero torque is in the range of $30 - 40\%$, lower than expected from Fig. 11.

A smaller series of 40 tex yarns were spun at 400 tpm (twist factor 80) from 20.2 μm wool to assess the effect of the yarn history and the test conditions on the torque/tension

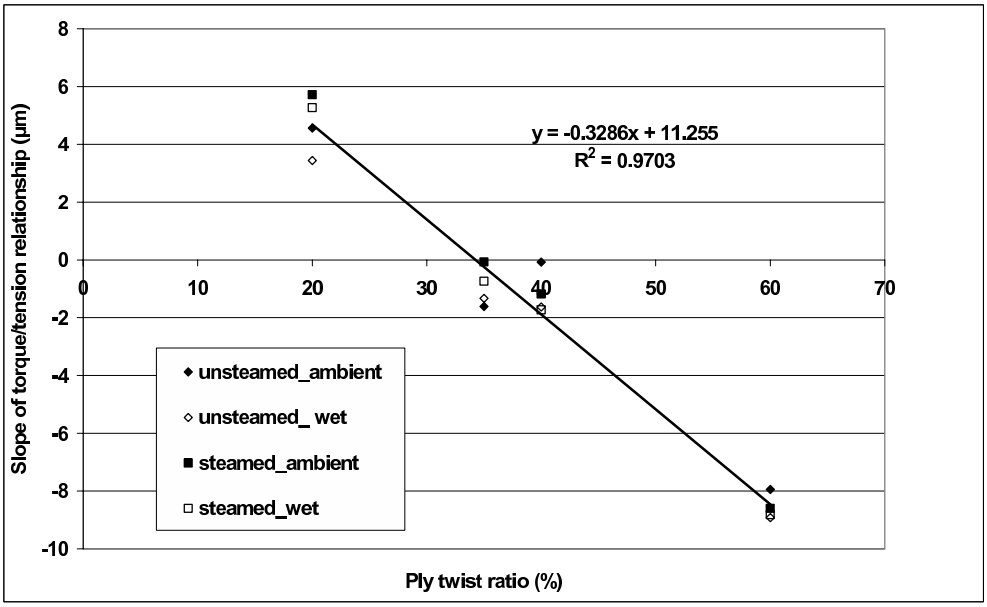

Figure 16: The effect of the yarn history and test conditions on the slope of the torque due to tension in R80/2 tex wool yarns.

relationship in plied yarns. The single yarns, either unsteamed or steamed, were plied into R80/2 yarns at different ply twist ratios and again unsteamed or steamed respectively and tested at ambient and wet conditions.

The effects of steaming the single and plied yarn and the test conditions on the slope data are shown in Fig. 16 and demonstrate again that the slope depends on the geometry and not on the fibre properties. The line of best fit intersects the x-axis at 34.3%, close to the predicted value of 33%.

By contrast the intrinsic torque varies significantly with the yarn history and the test conditions, as seen in Fig. 17.

The data shows a large effect of the ambient and wet test conditions on the torque values for the unsteamed yarn as expected from the change in the fibre and yarn mechanical properties. The calculated data in Figs 10 and 11 indicate that the unsteamed R80/2 tex yarn would have zero torque at a ply twist ratio near 69% and 45% when tested in ambient and wet conditions respectively. The experimental results for both situations in Fig. 17 show a zero torque near 60%. The model can be evaluated to assess the possible cause of these differences.

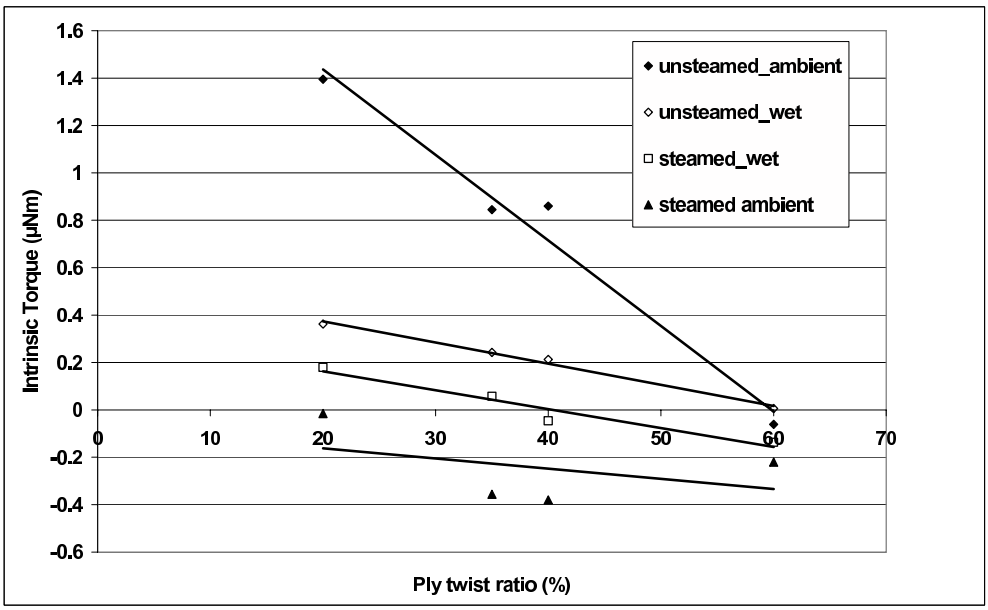

Figure 17: The effect of yarn history and test conditions on the intrinsic torque in R80/2 tex wool yarns.

The torque in spun unsteamed wool yarns decays with storage time. This reduction manifests itself in a reduction in twist-liveliness in freshly spun yarn. This is evident when the self-plying twist of a freshly spun yarn is measured with storage time. The self-plying twist of an 80 metric twist factor 50 tex yarn (358tpm) decays exponentially about 35 tpm per decade of time or 10% (Phillips et al. 2009) and if the self-plying twist is regarded as the balance point then clearly the ply twist for zero torque or balance decreases 10% per decade of storage time, i.e., from 50% to 40% in one decade. This may be a contributing factor to the values of about 60% measured for the unsteamed yarn in Fig. 17 compared to the predicted values of 69%. This reduction in the single and plied yarn torque was tested with the model by allowing for a reduction in the bending and torsional fibre moduli under ambient conditions. For example, a 25% reduction in the moduli showed that the intrinsic torque decreased by about 25% but the ply twist value for zero torque was largely unaffected. The 25% value was estimated as the decay that occurred in the 14 days of storage between spinning and testing the yarn torque in the unsteamed yarn using the published torque decay relationship in Phillips (2006).

Wetting of unsteamed yarn eliminates the storage history and cohesive set by raising the wool polymer above the glass transition temperature (Phillips 2006). However

setting of the wool polymer even under mild conditions is well-known. Again the effect of steam setting the singles and plied yarn can be modelled by allowing for a decrease in the wet fibre moduli due to stress relaxation from the steam setting treatment. The level of yarn set was estimated by measuring the set in a folded fabric sample that was set at the same time as the yarn was steamed. The set value of 47% was measured by relaxing the yarns removed from the fold in water at 20^o C for 30 mins. When the wet moduli were reduced by 50%, the wet intrinsic yarn torque decreased by 50% but again the ply twist ratio for zero yarn torque was largely unchanged. This suggests that although large changes in the fibre properties affect the yarn torque, other factors contribute to the balance point. Note that when fabric folds are stored for 14 days at ambient conditions to simulate storage of an unsteamed yarn and wet out, the set level is 0%.

Other variables in the model that can affect the ply twist for zero torque are the diameters of the yarn and the cylinder shown in Fig. 1a and the moment due to bending hysteresis M_s. A change of +20% or -20% of the yarn and cylinder diameters causes a small decrease and increase in the point of zero torque respectively.

The model proves useful for evaluating the role of the coercive bending moment M_s and shows that the data is sensitive to changes in M_s. In the model data shown in Figs 10 and 11 a constant value of 0.3 μNm was used for both the ambient and wet calculations. The unsteamed yarns have been spun under a small winding tension, say 20cN, and some of this will be cohesively set into the yarn on the package. When the yarn hank is wet for the torque measurement the yarn will shrink slightly and generate some bulk in the yarn which may actually reduce the yarn bending moment. If the bending moment is assumed to be zero then the balance point for the unsteamed yarn measured wet moves to 56%, closer to the value of 60% obtained experimentally.

On the other hand for yarns that are steamed on the package the shrinkage relaxation on wetting is less likely to occur due to the setting process and in fact the experimental results given earlier show that M_s is higher for the wet steamed yarns by about 26%. An increase in the wet bending moment from 0.3 μNm to 0.38 μNm lowers the ply twist for balance from 45% to 42% for the R80/2 yarn. If this is combined with a 50% reduction in the fibre mechanical properties due to setting the ply twist ratio for zero torque moves close to 36%. These values are quite similar to the experimental data in Figs 15 and 17 for the R62/2 and R80/2 yarns. These results implicate the role of the

bending hysteresis in the plied yarn behaviour.

Another set of results are shown in Fig. 17 for the steamed R80/2 yarns measured at ambient conditions and show negative torque values with a ply twist ratio for zero torque near 20%. This behaviour is also consistent with the model. The intrinsic torque in an unsteamed singles 50 tex yarn after one day relaxation was 2.27 μNm and 0.08 μNm after steaming when measured at ambient conditions. This indicates a reduction in the fibre moduli equivalent to 28 times and when this is placed into the model, the torque in the plied yarn is very low and negative for values of ply twist ratio above 30%.

In commercial practice a ply twist ratio of 55% (52-62% is given by Lee (1989)) is widely used as the balance point in worsted spun yarns with metric twist factors from 60 to 90 in the singles to avoid spirality in knitted single jersey fabric. This is on the lower range of the values predicted of ply twist ratio for zero torque and close to the value of 60% measured for the R80/2 unsteamed yarn. It is very interesting to note that the model data in Fig. 10 for ambient conditions predicts a small positive torque in the yarn at 55% whereas in the wet case a small negative torque is predicted at 55% ply twist. The choice of 55% essentially creates a plied yarn that has near to zero torque properties in ambient or wet conditions and this may provide a valuable compromise in commercial use. Another publication by IWS report (1996) recommends 60% ply twist ratio for two-ply machine knitting yarns and states that "To reduce the risk of stitch distortion, these yarns should not be steamed at all." and Oxtoby (1973) is quoted as recommending 67% as the two-ply twist ratio for balance.

The spirality of the plied yarns in Fig. 17 was measured (14 gauge single jersey fabrics, cover factor 1.2). For the steamed yarns in Fig. 17 the spirality measured as-knitted was close to zero at all ply twist ratios 20-60% implying yarn balance conditions and zero torque conditions whereas after wet relaxation of the knit fabric, spirality was generated, see Table 2. This is consistent with the changes in the torque in the plied yarn seen in Fig. 17. The link between yarn torque and spirality will be considered in another publication.

Another aspect of yarn management in manufacturing is the handling of twist lively yarns and the model suggests that in the range of ply twist ratio 50-55% the plied yarn torque is similar independent of the yarn twist and count for yarns spun from similar

Table 2: The spirality of R80/2 steamed yarns.

Ply twist ratio (%)	As knitted spirality (^{o})	Wet relaxed spirality (^{o})
20	0	15
40	0	6
60	−3	4

quality wool. This region of isotorque may allow a range of yarns to be processed in commercial practice without any modification of handling procedures. Further studies are needed to map the region of isotorque.

4 Conclusion

A mathematical analysis of the mechanical governing equations applying to the torsional behaviour of n-plied yarns under tension has been carried out. This analysis clearly shows that there are two components, a geometric component that determines the slope or gradient of the torque due to tension and a component that determines the yarn torque at zero applied tension (intrinsic torque) that depends on the fibre number, fibre moduli and diameter as well as the strand geometry. The effect of the ratio of the ply twist to the spinning twist of the single strands on the torque properties has been numerically analysed for two, three and four-ply yarns prepared from single 31 tex yarns and two-ply yarns from 40 and 80 tex singles.

The model was evaluated against torque due to tension data and intrinsic torque data measured from a series of two-ply yarns, R62/2 and R80/2. The model predicts that the slope of the torque due to tension changes from positive to negative at a ply twist ratio of 33 %. This agreed very well with the experimental data for R62/2 and R80/2 tex yarns. The model predicted that this ply ratio of 33% was independent of the fibre mechanical properties and the data for the torque of the 80 tex yarns (unsteamed and steamed) tested at ambient and wet conditions demonstrated this effect.

The model also predicts that the ply twist ratio for zero torque depends on the mechanical properties of the wool fibres with typical values of 65% and 45% in ambient and wet conditions respectively. The experimental values show similar differences ranging

from 60% to about 40% in ambient and wet conditions. The model has been able to demonstrate that the yarn bending moment can influence the ply twist ratio particularly when the yarn mechanical properties are affected by setting. The predicted values compare well with the experimental values using realistic values of yarn bending moments.

Appendix

Force and moment balance for the n-ply structure

In this Appendix we outline the derivation of the n-ply force and moment balance equations in somewhat more detail (Neukirch and van der Heijden, 2002). Let the path of the axis of the i-th strand ($i = 1, 2, \cdots, n$) be

$$\mathbf{R}_i = a\mathbf{e}_r{}^i + s\cos\theta\mathbf{k}, \tag{A.1}$$

where

$$\begin{aligned} \mathbf{e}_r{}^i &= \cos\left(\frac{i2\pi}{n} + \psi\right)\mathbf{i} + \sin\left(\frac{i2\pi}{n} + \psi\right)\mathbf{j}, \\ \mathbf{e}_\psi{}^i &= -\sin\left(\frac{i2\pi}{n} + \psi\right)\mathbf{i} + \cos\left(\frac{i2\pi}{n} + \psi\right)\mathbf{j}, \end{aligned} \tag{A.2}$$

are the unit basis vectors of a cylindrical coordinate system defined relative to the fixed Cartesian coordinate system with unit basis vectors $(\mathbf{i}, \mathbf{j}, \mathbf{k})$ (see Fig. 18). Since the centrelines lie on a cylinder of radius a (the ply radius), we have

$$\frac{d\psi}{ds} = \psi' = \frac{\sin\theta}{a}. \tag{A.3}$$

The tangent, normal and binormal unit vectors corresponding to this path are (Fig. 18a)

$$\begin{aligned} \mathbf{R}_i{}' &= \sin\theta\mathbf{e}_\psi{}^i + \cos\theta\mathbf{k}, \\ \mathbf{n}_i &= -\mathbf{e}_r{}^i, \\ \mathbf{b}_i &= -\cos\theta\mathbf{e}_\psi{}^i + \sin\theta\mathbf{k}. \end{aligned} \tag{A.4}$$

If we now assume that the torque $Q_i = Q_s$ and the tension $T_i = T_s$ in each strand have the same magnitudes we can write the force and moment equilibrium equations for the i-th strand as follows (Fig. 18b,c):

$$\begin{aligned} (T_s\mathbf{R}_i{}')' + \mathbf{V}_i{}' + \mathbf{F}_i &= \mathbf{0}, \\ (Q_s\mathbf{R}_i{}')' + \mathbf{M}_i{}' + \mathbf{R}_i{}' \times \mathbf{V}_i &= \mathbf{0}, \end{aligned} \tag{A.5}$$

where $\mathbf{F}_i$ is the force per unit length that the neighbouring strands exert on strand i, and that satisfies the following constraints:

$$\begin{aligned} \mathbf{F}_i \cdot \mathbf{R}_i{}' &= 0, \\ \sum_{i=1}^{N} \mathbf{F}_i &= \mathbf{0}. \end{aligned} \tag{A.6}$$

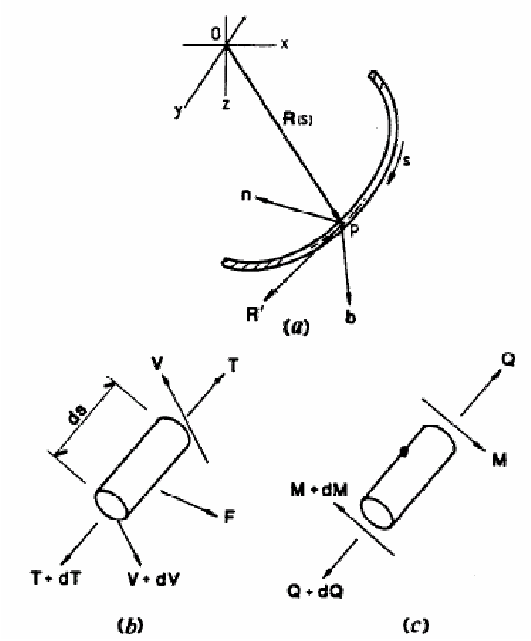

Figure 18: Schematic diagram showing the notation: (a) the tangent, principal normal and binormal unit vectors ($\mathbf{R}', \mathbf{n}, \mathbf{b}$, respectively), (b) the forces acting on the strand element, and (c) the moments acting on the strand element (figure borrowed from Fraser and Stump (1998b)).

Forming the vector product of $\mathbf{R}_i{}'$ with the second equation above we obtain

$$\mathbf{V}_i = Q_s(\mathbf{R}_i{}' \times \mathbf{R}_i{}'') + \mathbf{R}_i{}' \times \mathbf{M}_i{}', \tag{A.7}$$

where the constitutive equations (2.19) and (2.20) for the i-th strand are

$$\begin{aligned} Q_s &= \kappa_1 \tau_i + \kappa_3 {\tau_i}^3, \\ \mathbf{M}_i &= \left(M_s + B_s \frac{\sin^2\theta}{a} \right) \mathbf{b}_i, \end{aligned} \tag{A.8}$$

with $\mathbf{b_i}$ the binormal vector to the axis of strand i. Due to the symmetry of the n-ply structure the torsion

$$\tau_i = \phi' + \frac{\sin 2\theta}{2a} = \tau \tag{A.9}$$

is the same for all strands in the ply.

Making use of the above results, equation (A.7) can now be reduced to

$$\mathbf{V}_i = \left\{ Q_s \frac{\sin^2\theta}{a} - \left(M_s + B_s \frac{\sin^2\theta}{a} \right) \frac{\cos\theta \sin\theta}{a} \right\} \mathbf{b}_i. \tag{A.10}$$

Force and moment balance for the n-ply structure requires

$$\begin{aligned} T_0\mathbf{k} &= \sum_{i=1}^{n}(T_s\mathbf{R}_i{}' + \mathbf{V}_i), \\ Q_0\mathbf{k} &= \sum_{i=1}^{n}[\mathbf{M}_i + Q_s\mathbf{R}_i{}' + T_s(\mathbf{R}_i \times \mathbf{R}_i{}') + (\mathbf{R}_i \times \mathbf{V}_i)], \end{aligned} \tag{A.11}$$

so that finally we obtain

$$T_0 = n\left\{T_s\cos\theta + Q_s\frac{\sin^3\theta}{a} - \left(M_s + B_s\frac{\sin^2\theta}{a}\right)\frac{\cos\theta\sin^2\theta}{a}\right\}, \tag{A.12}$$

$$Q_0 = n\left\{T_s a\sin\theta + Q_s cos^3\theta + \left(M_s + B_s\frac{\sin^2\theta}{a}\right)\sin\theta(1+\cos^2\theta)\right\}. \tag{A.13}$$

References

Bennett, J.M. and Postle, R. (1979a) 'A study of yarn torque and its dependence on the distribution of fibre tensile stress in the yarn. Part I: Theoretical analysis.' *J. Text. Inst.* **70**, 121–132.

Bennett, J.M. and Postle, R. (1979b) 'A study of yarn torque and its dependence on the distribution of fibre tensile stress in the yarn. Part II: Experimental.' *J. Text. Inst.* **70**, 133–141.

Booth, J.E. (1975) *Textile Mathematics, Vol 2,* Textile Institute, Manchester.

Dhingra, R.C. and Postle, R., (1976) The Bending and Recovery Properties of Continuous Filament and Staple Fibre Yarns, *J. Text. Inst.*, **67**, 426-433.

Fraser, W.B. and Stump, D.M. (1998a) 'The equilibrium of the convergence point in two strand yarn plying.' *Int. J. Solids and Structures.* **35**, 285–298.

Fraser, W.B. and Stump, D.M. (1998b) 'Twist in balanced ply structures.' *J. Text. Inst.* **89**, 485–497.

Lee, C.S.P. (1989) 'Quality control aspects of wool processing.' *IWS Tech. Group report.* Section 2.3.2.

Love, A.E.H. (1927) *A Treatise on the Mathematical Theory of Elasticity,* 4th ed. Cambridge University Press, Cambridge (Chapter 18).

Ly, N.G. and Denby, E.F. (1984) 'Bending rigidity and hysteresis of wool worsted yarn.' *Text. Res. J.*, **54**, 180–187.

Mitchell, P., Naylor, G. R. S. and Phillips, D. G. (2006) 'Torque in worsted wool yarns.' *Text. Res. J.*, **76**, 169–180.

Mitchell, T.W. and Feughelman, M. (1965) 'The bending of wool fibers.' *Text. Res. J.*, **35**, 311–314.

Neukirch, S. and van der Heijden, G.H.M. (2002) 'Geometry and mechanics of uniform n-plies: from engineering ropes to biological filaments.' *J. Elasticity*, **69**, 41–72.

Oxtoby, E., (1973) The Wira Textile Data Book. Rae, A and Brace, R., B40

Phillips, D.G. (2006) 'Torque in Twisted Structures.' Proc. Autex World Conference, NCSU, Rayleigh.

Phillips, D.G., Hair, J., Marsh, J.A. and Staynes, L.M. (2009) 'The Effect of Physical Ageing on Torque in Worsted Spun Yarns.' *Fibers and Polymers.* (in press)

Platt, M.M., Klein, W.G. and Hamburger, W.J. (1958) 'Mechanics of elastic performance of textile materials Part XIII: Torque development in yarn systems: singles yarn.' *Text. Res. J.,* **28**, 1–14.

Platt, M.M., Klein, W.G. and Hamburger, W.J. (1959) 'Space density of fibers in idealized singles yarn', *Text. Res. J.,* **29**, 592–593.

Speakman, J.B. (1929) 'The rigidity of wool and its change with adsorption of water vapour.' *Trans Faraday Soc.,* **25**, 92–103.

Thompson, J.M.T., van der Heijden, G.H.M. and Neukirch, S. (2002) 'Supercoiling of DNA plasmids: mechanics of the generalized ply.' *Proc. Roy. Soc. Lond.* A**458**, 959–985.

Tran C.D., Phillips, D.G. and van der Heijden G.H.M. (2006) 'Issues in processing unstable twisted fibre assemblies.' in *Proc. of the 4th International Simulation Conference*, 325–329. The European Technology Institute and The European Simulation Society, Palermo, Italia.

Tran, C.D. and Phillips, D.G. (2007) 'Predicting torque of worsted singles yarn using an efficient radial basis function network-based method.' *J. Text. Inst.* **98**, 387–396.

Tran, C.D. and Phillips, D.G. (2008) 'Modelling and Performance of Multi-strand Spun Yarns including two-strand Sirospun.' Proc. Fiber Soc., Mulhouse.

Tran C.D., van der Heijden G.H.M. and Phillips, D.G., (2008) 'Application of topological conservation to model key features of zero-torque multi-ply yarns', *J. Text. Inst.* **99**, 325–337.